Journal of Plankton Research

plankt.oxfordjournals.org

Costa Rica Dome: Flux and Zinc Experiments

Net biogenic silica production and the contribution of diatoms to new production and organic matter export in the Costa Rica Dome ecosystem

JEFFREY W. KRAUSE[1,2]*, MICHAEL R. STUKEL[3], ANDREW G. TAYLOR[4], DARCY A. A. TANIGUCHI[4,5], ALAIN DE VERNEIL[4] AND MICHAEL R. LANDRY[4]

[1]DAUPHIN ISLAND SEA LAB, 101 BIENVILLE BLVD, DAUPHIN ISLAND, AL 36528, USA, [2]UNIVERSITY OF SOUTH ALABAMA, LIFE SCIENCES BUILDING ROOM 25, MOBILE, AL 36688, USA, [3]FLORIDA STATE UNIVERSITY, P.O. BOX 3064520, TALLAHASSEE, FL 32306-4520, USA, [4]SCRIPPS INSTITUTION OF OCEANOGRAPHY, 9500 GILMAN DR., LA JOLLA, CA 92093-0227, USA AND [5]MASSACHUSETTS INSTITUTE OF TECHNOLOGY, 77 MASSACHUSETTS AVENUE, BUILDING 54-1511A, CAMBRIDGE, MA 02142, USA

*CORRESPONDING AUTHOR: jkrause@disl.org

We determined the net rate of biogenic silica ($bSiO_2$) production and estimated the diatom contribution to new production and organic matter export in the Costa Rica Dome during summer 2010. The shallow thermocline significantly reduces $bSiO_2$ dissolution rates below the mixed layer, leading to significant enhancement of $bSiO_2$ relative to organic matter (silicate-pump condition). This may explain why deep export of $bSiO_2$ in this region is elevated by an order of magnitude relative to comparable systems. Diatom carbon, relative to autotrophic carbon, was low ($<3\%$); however, the contribution of diatoms to new production averaged 3 and 13% using independent approaches. The 4-old discrepancy between methods may be explained by a low average C:Si ratio (~1.4) for the net produced diatom C relative to the net produced $bSiO_2$. We speculate that this low production ratio is not the result of reduced C, but may arise from a significant contribution of non-diatom silicifying organisms to $bSiO_2$ production. The contribution of diatoms to organic matter export was minor (5.7%). These results, and those of the broader project, suggest substantial food-web transformation of diatom organic matter in the euphotic zone, which creates enriched $bSiO_2$ relative to organic matter within the exported material.

KEYWORDS: diatom; biogenic silica production; vertical flux; new production

INTRODUCTION

Despite the regular occurrence of elevated biomass for high-trophic-level organisms, autotrophic biomass and published rates of primary production in the Costa Rica Dome (CRD) are not particularly high (Pennington *et al.*, 2006). Even though large phytoplankton (e.g. diatoms) are assumed to dominate systems that support high-trophic-level biomass, the importance of the picophytoplankton contribution to autotrophic biomass and primary production in the CRD has been known for decades (Li *et al.*, 1983). Specifically, the abundance of the picocyanobacteria from the genus *Synechococcus* in the CRD is among the highest observed in the open ocean (Campbell and Vaulot, 1993; Durand *et al.*, 2001; Stukel *et al.*, 2013a). Using biogenic silica ($bSiO_2$) as a proxy, the diatom biomass in the CRD (Franck *et al.*, 2003) is more similar to the subtropical gyres (Krause *et al.*, 2009a; Brzezinski *et al.*, 2011) than coastal systems that support similar high-trophic-level organisms (Brzezinski *et al.*, 2003; Krause *et al.*, 2013a). Counterintuitive to the low diatom biomass and dominance by the picoplankton, model results from Honjo *et al.* (Honjo *et al.*, 2008) show that rate of $bSiO_2$ export at 2 km in the CRD is similar to the highest rates observed in low-latitude open-ocean systems (e.g. equatorial Pacific, Arabian Sea). These enhanced export rates could be sustained with very high export efficiency by diatoms, a larger contribution by other siliceous groups (e.g. radiolarians), a regional difference in the rate of $bSiO_2$ remineralization or some combination of the three. Validating these model results requires understanding of the upper-water-column Si-cycling as these collective processes ultimately sustain export.

Currently, only one regional dataset for particulate $bSiO_2$ and Si uptake is available in the primary literature (Franck *et al.*, 2003). It consists of one multi-day grow-out experiment in a shipboard deck incubator designed to understand the effects of trace-metal limitation on nutrient uptake. Therefore, no data describing the spatial, temporal or vertical variability in $bSiO_2$ and its rate of production are published for the CRD. Additionally, no direct or indirect measurements of $bSiO_2$ dissolution are available for this region, and the balance between production and loss rates for $bSiO_2$ in the euphotic zone, which is essential to understand the potential fraction of $bSiO_2$ available for export to the ocean interior, is unknown. Data from the eastern equatorial Pacific suggest that over 65% of the $bSiO_2$ produced in the euphotic zone dissolves there (Krause *et al.*, 2010a). If the CRD does sustain such high $bSiO_2$ export to the deep ocean (e.g. 2- to 5-fold higher than the eastern equatorial Pacific, Honjo *et al.*, 2008), then considerably lower $bSiO_2$ dissolution would be expected in the euphotic zone.

Enhancements of diatom biomass and productivity in the open ocean have been observed to transform deep-water systems. For example, eddies or fronts can lead to enhancement of diatom biomass, which is typically very low in open-ocean regions, and can sustain biomass of higher trophic levels (Goldthwait and Steinberg, 2008; Landry *et al.*, 2008, 2012). Whereas similar processes may occur in the CRD, there has been no intensive examination of the rates of diatom production and the potential efficiency with which this production might contribute to other processes. Indeed, even in a relatively well-studied region like the equatorial Pacific, only two estimates of the diatom contribution to primary and new production have been made (Leynaert *et al.*, 2001; Krause *et al.*, 2011), and there is still a gap between understanding their roles in organic matter production and the food-web processes controlling diatom contributions to organic matter export.

Under steady-state assumptions, net production of $bSiO_2$ is fueled by new silicic acid (Brzezinski *et al.*, 2003), and like new N-based production (Dugdale and Goering, 1967), this material can be exported from the euphotic zone versus being remineralized within it. Organic forms of C and N associated with the net $bSiO_2$ produced can be passed to higher trophic levels; however, since consumed $bSiO_2$ is not assimilated by grazers, its likely fate is export in zooplankton fecal pellets (Krause *et al.*, 2010a). With an understanding of diatom cellular Si:C and Si:N ratios, Si-based rates can be converted to diatom-specific C and N rates; therefore, net $bSiO_2$ production can be used to infer the amount of diatom organic matter which can be passed to higher trophic levels and/or lost from the euphotic zone through export.

The goals of this study are (i) to understand the balance between $bSiO_2$ production and dissolution to determine whether the water-column processes can potentially support high $bSiO_2$ export to the CRD mesopelagic, and (ii) to estimate the regional contribution of diatoms to new production and organic matter export in the upper-water column. To meet the first goal, we report the net rate of $bSiO_2$ production, which reflects the balance between gross $bSiO_2$ production and dissolution (i.e. net production = gross production − gross dissolution), such that positive net production indicates that gross production exceeds gross dissolution of $bSiO_2$. For the second goal, the disparity between the contribution of diatoms to new production and organic matter export, which would be equal if diatoms settle as intact cells (i.e. organic matter not assimilated into the food web), can shed light on the relative importance of food-web transformation of diatom organic matter prior to its export from the euphotic zone.

METHODS

Sampling

This present data was generated during the CRD FLUx and Zinc Experiments (FLUZiE) cruise from 22 June to 25 July 2010 aboard R/V *Melville*. As described in greater detail elsewhere (Landry *et al.*, this issue-a), plankton community dynamics, food-web fluxes and biogeochemical relationships were studied in 4- or 5-day Lagrangian-style experiments (termed "cycles") beginning at five different starting locations in the CRD. During each cycle, daily water-column sampling and rate measurements were carried out following a satellite-tracked drifter with a holey-sock drogue, centered at 15 m (Landry *et al.*, 2009). Samples to measure biological process rates were incubated *in situ* for 24 h at the depth of sample collection on a line attached below the drift array. A second drift array with VERTEX-style acrylic sediment traps at two depths (90 or 100 m and 150 m) was deployed at the start of each cycle and recovered at the end to determine mean export rates during the experiment (Stukel *et al.*, 2013b).

Samples for standing stock and biological rate determinations were collected during early morning hydrocasts (~02:00 local time) using Niskin bottles on a CTD rosette. Hydrocasts were taken within ~100 m of the primary drift array; profiles extended to ~500 m and Niskin bottles were filled from the upper 100 m. Samples for rate measurements were taken each day (3 days for Cycle 1; 4 days for Cycles 2–5), except for the last day, which only sampled for final measurement of standing stocks. Experimental bottles were filled directly from the rosette bottles, placed into mesh bags, secured to the array and the array deployed, all completed in ~2.5 h of sample collection and prior to local sunrise. Experiments on adjacent days were set up first on deck, then the array was recovered, the mesh bags switched and the array redeployed in ~20 min. Incubated samples were processed immediately after array recovery, and sediment-trap samples were processed within a few hours.

Standing stocks

Macronutrients and biogenic particles were sampled at the same depths and hydrocasts as the rate experiments. Water for macronutrients was filtered directly from the Niskin bottles through a 0.1-μm capsule filter (Suporcap), and the filtrate was immediately frozen at $-20°C$. Nutrient samples (NO_3^-, NO_2^-, PO_4^{3-}, $Si(OH)_4$) were analyzed by flow injection on shore at the Analytical Facility of the Marine Science Institute, University of California at Santa Barbara. Seawater samples (1.0 L) for $bSiO_2$ analysis were filtered through 0.6-μm polycarbonate

membranes, placed in cryovials, and dried in an oven for ~24 h. On shore, quantification of $bSiO_2$ concentration was done using an NaOH digestion procedure (Brzezinski and Nelson, 1995) in Teflon tubes, which provides low and stable blanks (Krause *et al.*, 2009b). Concentration of chlorophyll *a* (Chl a) was determined at sea on a Turner 10 AU fluorometer after filtering 250-mL samples through glass fiber filters, and extracting in 90% acetone in the dark at $-20°C$ for 24 h (Strickland and Parsons, 1972). For Cycles 2–5, taxon-grouped abundances and biomasses of eukaryotic nano- and microplankton, including diatoms, were quantified by image analysis using epifluorescence microscopy (Taylor *et al.*, this issue) and picophytoplankton (*Prochlorococcus*, *Synechococcus*, picoeukaryotes) biomass by flow cytometry (Selph *et al.*, this issue). Here, we report the diatom carbon and percent contribution to the total autotrophic C.

Production and export rates

The rate of net $bSiO_2$ production was determined by the difference between $bSiO_2$ concentration in initial whole seawater samples (no nutrient amendments or dilution, processed immediately) relative to those incubated for 24 h on the drift array. For water budget reasons, only single initial and final bottles were analyzed at each of eight depths in the profiles. Replication was thus provided by independent measurements at the same depths during successive days of the cycles. In small-volume bottles (i.e. <4 L) with a high surface-area to volume ratio, $bSiO_2$ adsorption to the bottle walls can be quantitatively significant, and without correction can lead to systematic errors in the calculated net rates (Krause *et al.*, 2010b). To minimize these effects for $bSiO_2$ filtrations (i.e. initial or final), the bottles were rinsed three times with ~50 mL of 0.1-μm filtered seawater per rinse, and the rinse volume was added to the volumes filtered (Krause *et al.*, 2010b, 2013b). These initial and final $bSiO_2$ concentrations were then used to calculate the net rates of $bSiO_2$ production (ρ_N) that occurred during the 24-h incubations. During the cruise, environmental variability in the [$bSiO_2$] measurement was assessed by taking replicate samples ($n = 9$). For this particular sample set, the measured [$bSiO_2$] was 116 ± 10 nmol Si L^{-1}. The coefficient of variation was 8.8% and is well within the range of replicates for previous studies (Krause *et al.*, 2010b, 2013b).

Vertical integrals for biomass (e.g. $bSiO_2$, Chl a, Diatom C) and net production (ρ_N) were done between the surface and 80 m using the trapezoidal approach. Average specific rates of ρ_N were derived as V_{NET} (day^{-1}) = $\rho_N \times$ [$bSiO_2$]$^{-1}$. To estimate the average specific V_{NET} within the upper 80 m ($\int$Ave V_{NET}), V_{NET} was integrated and the summed quantity was divided by the depth of integration (80 m) as done previously (Krause *et al.*, 2010a).

The average contribution of Diatom C to total autotrophic C throughout the upper 80 m was calculated similarly.

Concurrent measurements of $^{15}NO_3^-$ uptake are used to estimate the contributions of diatoms to the rate of new production during the FLUZiE cruise. ^{15}N uptake experiments were conducted with water samples from the same CTD cast as those used for $bSiO_2$ net uptake and ρ_N assessments and incubated *in situ* at the same depth and for the same time. Specific information regarding the methods and results of these experiments can be found elsewhere (Stukel *et al.*, this issue).

Particle export was measured using a free-drifting sediment-trap array (Krause *et al.*, 2009b; Stukel *et al.*, 2013b). Prior to deployment, acrylic collector tubes fitted with entrance baffles comprised of 14 smaller tubes with tapered edges were filled with a saltwater brine (0.1-μm filtered surface seawater, amended with 50 g L^{-1} NaCl and 1% final concentration formalin). Tubes were deployed at two depths (90 or 100 m, and at 150 m) for ~4 days of collection. After recovery, samples were filtered through a 200-μm filter, and swimming zooplankton were sorted microscopically and removed from the >200-μm fraction, which was then recombined with the <200-μm fraction. Three different tubes thus cleared of swimmers were subsampled using a rotary splitter for measurement of [$bSiO_2$], as described above, and calculation of $bSiO_2$ export (ρ_E). Sediment-trap subsamples for particulate organic carbon (POC) were analyzed on a CHN Analyzer at the Scripps Institution of Oceanography Analytical Facility. Concurrent ^{234}Th analyses made with these trap

arrays have consistently shown no consistent over- or under-collection bias (Stukel *et al.*, 2013b, this issue).

RESULTS

Hydrography and standing stocks

Locations of the Lagrangian cycle experiments were chosen in relation to the core of the CRD as determined from satellite images of [Chl a], when available, and ADCP mapping prior to the cycle work. Post-cruise assessment of sea-surface temperature (SST) from weekly composite *Advanced Very High Resolution Radiometer (AVHRR)* data clearly shows the low SST signature of the CRD centered at ~9°N, 90°W (Fig. 1). Cycle 1 was located outside of the dome, in southward flowing warm waters close to the coast of Costa Rica (Landry *et al.*, this issue-a), Cycle 2 was located slightly southeast of the SST minimum. Cycle 3 was northwest and separated from the colder SST of the CRD by southward intrusion of a warm-SST filament. Cycle 4 was within the cool SST region of the CRD core and Cycle 5 started east of the core moving quickly eastward toward the coast in the North Equatorial Counter Current.

The thermal characteristics of the upper-water column were similar among cycles (Fig. 2A). The mixed layer depth (MLD) was shallowest during Cycle 3 (~12 m) and deepest during Cycle 5 (~30 m). The other three cycles showed very similar MLD (18–22 m, Table I). Below the MLD, a sharp thermocline was observed between
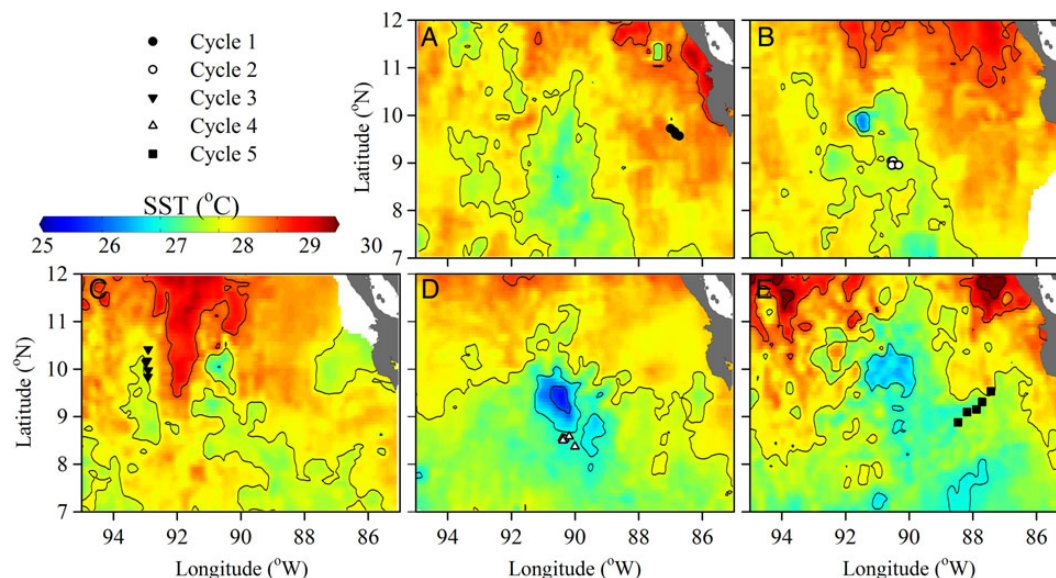

Fig. 1. Cruise station locations (symbols, see legend) and regional weekly composite AVHRR Global Area Coverage SST for (**A**) Cycle 1: 24 June SST, (**B**) Cycle 2: 1 July SST, (**C**) Cycle 3: 8 July SST, (**D**) Cycle 4: 15 July SST and (**E**) Cycle 5: 22 July SST. AVHRR data were accessed from National Oceanic and Atmospheric Administration (NOAA) OceanWatch Central Pacific Live Access Server (http://oceanwatch.pifsc.noaa.gov/).
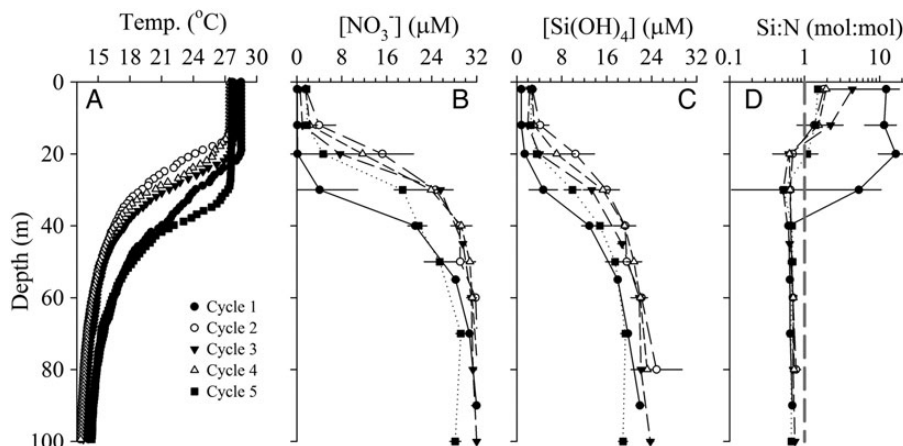
Fig. 2. Vertical profiles for (**A**) temperature, (**B**) nitrate concentration, (**C**) silicic acid concentration and (**D**) silicic acid:nitrate molar ratio (reference line Si:N = 1) in the upper 100 m. Data from all cycle hydrocasts and Niskin samples were averaged per depth (error bars are standard deviations).

~20 and 60 m, such that water at or deeper than 60 m was >10°C cooler than surface waters at all stations.

Nutrients were depleted in the surface waters and increased rapidly in the shallow thermocline (Fig. 2B and C). Mixed-layer concentrations of nitrate varied from low values of <0.1 μM and ~0.7 μM for Cycles 1 and 3, respectively, to 3.4−5.2 μM for the other cycles (Table I). Within the thermocline, nitrate increased rapidly, such that concentrations were >28 μM at or deeper than 60 m. Dissolved phosphate showed similar behavior to nitrate, with an N:P ratio less than typical Redfield (<16, data not shown) which may be a result of denitrification in the source-water (e.g. Devol, 2008). The vertical structure for dissolved silicic acid was also similar to nitrate (Fig. 2C) with average mixed-layer concentration lower for Cycles 1 (1.0 μM) and 3 (2.2 μM), and higher, comparable concentrations for the other cycles (3.5−4.3 μM, Table I). In the thermocline, silicic acid concentrations ranged from 16 to 24 μM between 40 and 100 m, and deeper concentrations were typically ~70% of those for nitrate. For both nitrate and silicic acid, the strong and shallow thermocline resulted in high variability in mixed-layer nutrient concentrations (Table I). Comparing the ratios of silicic acid to nitrate shows a strong vertical trend of high Si:N in the surface to ratios <1 below 20 m (Fig. 2D). Especially high Si:N (5−16) was observed in the upper 30 m during Cycle 1, and values between 2 and 4 were also observed in the upper 12 m during Cycle 3 (off-scale points not shown in Fig. 2D). All the high Si:N values were driven by intense nitrate draw down, as opposed to especially high concentrations of silicic acid (Fig. 2B and C).

Algal biomass proxies showed similar vertical patterns within and between the different cycles. [Chl a] displayed subsurface maxima in all cycle profiles, typically at or below the base of the mixed layer (Fig. 3D). The mean mixed-layer [Chl a] was highest during Cycle 4 (~0.4 μg L^{-1}) and lowest for Cycle 5 (~0.2 μg L^{-1}). [Chl a] declined in the thermocline and typically was <0.1 μg L^{-1} below 60 m. As with [Chl a], the highest [bSiO$_2$] was observed during Cycle 1, with peak subsurface value of ~350 nmol Si L^{-1} near the base of the mixed layer (Fig. 3A). The [bSiO$_2$] profiles were similar among Cycles 2−5, with subsurface maxima near the base of the mixed layer, and peak values between 125 and 250 nmol Si L^{-1}. Also similar to [Chl a], [bSiO$_2$] was lowest during Cycle 5 (20−25% of maximum values during Cycle 1), with near uniform values between 60 and 90 nmol Si L^{-1} in the upper 100 m. Like [bSiO$_2$], [Diatom C] showed a subsurface maximum (~900− 1200 ng L^{-1}), during Cycles 3 and 5 (Fig. 3C). In contrast, [Diatom C] was highest in near-surface samples, not subsurface maxima, during Cycles 2 (~300 ng L^{-1}) and 4 (~900 ng L^{-1}); however, there was also a high surface value observed during Cycle 5 (~900 ng L^{-1}). In addition, microscopically estimated [Diatom C] declined faster than [bSiO$_2$] with depth, typically reaching near zero values at depths >60 m, but higher [Diatom C] persisted deeper during Cycle 5 (Fig. 3C).

Vertical integrations of Chl a were similar among most cycles (Table I), ranging from a low of 15.3 mg m^{-2} (Cycle 4) to the high of 20.3 mg m^{-2} (Cycle 1). ∫bSiO$_2$ and ∫Diatom C were both more variable. During Cycle 1, the ∫bSiO$_2$ of 16.7 ± 1.1 mmol Si m^{-2} was nearly twice that of any other cycle. Similar to other variables, ∫bSiO$_2$ for Cycles 2, 4 and 5 was most similar (range 6.1− 7.1 mmol Si m^{-2}), and Cycle 3 was modestly enhanced (9.6 ± 1.2 mmol Si m^{-2}). ∫Diatom C had a larger relative range than ∫Chl a or ∫bSiO$_2$, with Cycle 2 having the lowest integrated biomass (6.8 ± 5.1 mg C m^{-2}, Table I), Cycles 3 and 4 being enhanced by ~3-fold, and Cycle 5

Table I: Cruise station data

Cycle	Cast	MLD (m)	ML-Ave NO_3^- (µM)	ML-Ave $Si(OH)_4$ (µM)	∫Chl (mg m^{-2})	∫Diatom C (mg m^{-2})	Ave ∫Diatom C: ∫Auto C (%)	∫bSiO$_2$ (mmol Si m^2)	∫ρ$_N$ (mmol Si m^2 day^{-1})	∫Ave V_{NET} (day^{-1})	ρ$_E$ ~100 m (mmol Si m^2 day^{-1})	ρ$_E$ 150 m (mmol Si m^2 day^{-1})
1	3	20	0.12 ± 0.04	0.95 ± 0.23	18.9	~	~	15.7	2.3	0.10	5.90 ± 0.01	6.16 ± 0.12
	6	23	0.10 ± 0.14	1.16 ± 0.66	19.3	~	~	18.3	−0.7	−0.05		
	9	20	0.08 ± 0.03	1.08 ± 0.46	22.4	~	~	16.2	4.2	0.13		
	11	24	0.05 ± 0.02	0.86 ± 0.12	20.7	~	~	16.8	~	~		
	Ave	21.6 ± 2.0	0.09 ± 0.13	1.01 ± 0.78	20.3 ± 1.6	~	~	16.7 ± 1.1	1.9 ± 2.5	0.06 ± 0.10		
2	25	20	7.47 ± 8.74	6.12 ± 4.95	19.7	0.8	0.1%	6.1	1.0	0.15	2.26 ± 1.81	1.10 ± 0.19
	30	14	4.85 ± 4.70	4.55 ± 2.87	18.8	5.4	0.4%	6.1	−0.6	−0.08		
	33	19	1.61 ± 0.11	2.88 ± 0.01	16.7	7.7[a]	0.4%	7.4	1.9	0.23		
	37	14	3.69 ± 3.11	3.79 ± 1.62	16.7	5.4	0.8%	6.6	0.1	0.05		
	40	22	3.95 ± 4.62	4.23 ± 2.40	13.4	14.7[a]	0.9%	5.5	~	~		
	Ave	17.7 ± 3.6	4.31 ± 9.03	4.31 ± 5.38	17.0 ± 2.4	6.8 ± 5.1	0.5% ± 0.3%	6.3 ± 0.7	0.6 ± 1.1	0.09 ± 0.14		
3	41	17	0.57 ± 0.25	2.51 ± 0.57	10.7	8.8	1.0%	11.2	3.5	0.22	1.77 ± 0.76	2.07 ± 0.28
	45	17	0.63 ± 0.13	3.02 ± 1.93	14.9	46.1	3.2%	10.6	2.4	0.16		
	48	3	0.86	1.95	17.7	12.1	1.3%	9.2	1.6	0.16		
	53	8	0.54	1.77	16.6	12.8	1.2%	8.7	1.1	0.13		
	56	14	1.05 ± 0.70	1.54 ± 0.19	21.7	11.1	1.9%	8.3	~	~		
	Ave	11.5 ± 5.9	0.73 ± 1.20	2.16 ± 3.39	16.3 ± 4.0	18.2 ± 15.7	1.7% ± 0.9%	9.6 ± 1.2	2.2 ± 1.0	0.17 ± 0.04		
4	57	20	3.42 ± 3.13	3.41 ± 0.85	12.3	8.5	0.5%	6.2	0.5	0.02	1.25 ± 0.37	1.04 ± 0.15
	61	22	4.17 ± 5.49	3.58 ± 2.18	12.9	12.1	1.1%	6.6	0.4	0.07		
	64	22	4.11 ± 4.71	3.65 ± 1.99	18.2	30.1	3.3%	6.3	2.8	0.50		
	67	14	2.87 ± 1.99	3.50 ± 0.69	13.7	20.7	1.3%	7.7	2.3	0.35		
	70	18	2.67 ± 0.59	3.24 ± 0.54	19.5	31.4	1.3%	9.0	~	~		
	Ave	19.1 ± 3.3	3.44 ± 7.24	3.47 ± 3.10	15.3 ± 3.3	20.5 ± 10.3	1.5% ± 1.1%	7.1 ± 1.2	1.5 ± 1.2	0.24 ± 0.23		
5	71	22	6.05 ± 7.04	4.16 ± 2.37	13.6	28.7	1.9%	6.6	2.9	0.48	1.24 ± 0.20	1.05 ± 0.23
	75	34	6.20 ± 8.74	4.55 ± 4.07	12.5	~	~	5.1	2.5	0.57		
	78	33	5.95 ± 7.45	4.40 ± 2.70	13.1	~	~	6.5	2.8	0.44		
	82	28	2.08 ± 0.61	2.38 ± 0.13	15.7	~	~	5.5	2.8	0.44		
	85	32	5.69 ± 8.40	3.97 ± 3.31	25.8	30.1	1.4%	6.1	~	~		
	Ave	29.6 ± 4.9	5.19 ± 13.9	3.89 ± 5.77	16.2 ± 5.5	29.4 ± 0.7	1.7% ± 0.4%	6.0 ± 0.7	2.8 ± 0.2	0.48 ± 0.06		

Mixed-layer average (ML-Ave) nutrients: nitrate (NO_3^-) and silicic acid ($Si(OH)_4$). Water-column integrated (surface−80 m) Chl a (∫Chl), diatom carbon (∫Diatom C), proportion of diatom C to autotrophic carbon (∫Diatom C: ∫Auto C), biogenic silica (∫bSiO$_2$), net production rate for biogenic silica (∫ρ$_N$) and the average surface−80 m biomass-normalized rate for ρ$_N$ (∫Ave V_{NET}). bSiO$_2$ export rates (ρ$_E$) are reported for 100 and 150 m traps. Average values (± SD) are listed for each cycle. "~" denotes no samples taken for a particular profile.
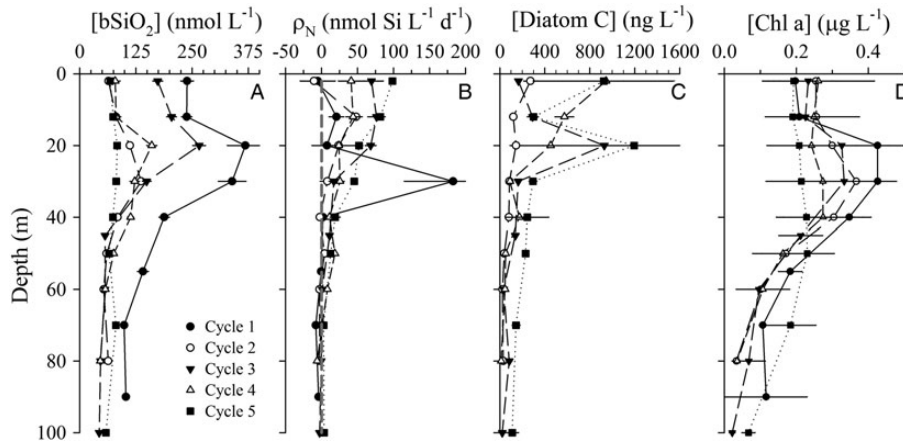[a]Diatom data only to 60 m.

Fig. 3. Vertical profiles of diatom standing stock and production rates in the upper 100 m for Cycles 1−5. (**A**) $bSiO_2$ concentration, (**B**) net $bSiO_2$ production (gray dashed line = 0), (**C**) Diatom carbon (no data for Cycle 1) and (**D**) Chl a concentration. Values are averages for all hydrocasts during a particular cycle (error bars = standard deviation). *Note*: for ease of viewing, the *x*-axis scale in (B) is truncated and does not show the full upper error range for subsurface maximum value.

having the highest and least variable biomass (29.4 ± 0.7 mg C m^{-2}, Table I). When the contributions of [Diatom C] to total autotrophic C were averaged for the upper 80 m, diatoms accounted for a low proportion of total autotrophic C during all cycles, 0.5−1.7% (Table I).

Net $bSiO_2$ production and export

The average net rate profiles of $bSiO_2$ production (ρ_N) were relatively similar among cycles (Fig. 3B). Overall, 72% of all ρ_N measurements were positive (i.e. gross $bSiO_2$ production > gross $bSiO_2$ dissolution), as were the average (24.3 nmol Si L^{-1} day^{-1}) and median (10 nmol Si L^{-1} day^{-1}) values for the dataset. However, ρ_N estimates varied greatly among depths, with the highest 10% of ρ_N values ranging from 93 to 415 nmol Si L^{-1} day^{-1} and the lowest 10% of ρ_N values ranging from −116 to −14 nmol Si L^{-1} day^{-1} (individual profiles not shown). Among cycles, higher positive ρ_N values were typical of surface waters with a more gradual decline to near zero rates at or deeper than 60 m (Fig. 3B). This general pattern differed in Cycle 1, where a 30-m subsurface maximum in average ρ_N was observed. This depth had the highest single ρ_N measurement in the dataset, but the vertical trend was robust, as removing this single value still yielded the subsurface maximum in the average profile of ρ_N for the cycle.

When vertically integrating in the upper 80 m, 17 of 19 profiles had positive $\int\rho_N$. The only statistically significant difference among individual cycles (i.e. $P < 0.01$) was between Cycle 2 (0.6 ± 1.1 mmol Si m^{-2} day^{-1}) and Cycle 5 (2.8 ± 0.2 mmol Si m^{-2} day^{-1}), the minimum and maximum cycles for $\int\rho_N$. However, the upper 80-m averages for specific rates of net $bSiO_2$ production ($\int$Ave V_{NET}) were more variable among cycles (ANOVA single

factor, $P < 0.005$, Table I). $\int$Ave V_{NET} was lowest during Cycles 1 and 2 (0.06 and 0.09 day^{-1}, respectively), increased by nearly 3-fold during Cycles 3 and 4 (0.17 and 0.24 day^{-1}, respectively), and more than doubled again for Cycle 5 (0.48 day^{-1}). Based on $\int$Ave V_{NET} data, the net doubling times for $bSiO_2$, calculated as $\int bSiO_2/\int\rho_N$ for the upper 80 m, were longest and most variable for Cycles 1 and 2 (8.7 ± 6.5 and 10.8 ± 10.3 days, respectively) and shortest (2.2 ± 0.1 days) during Cycle 5 (Fig. 4). Cycles 3 and 4 were intermediate with similar variability (4.4 ± 1.1 and 4.8 ± 2.0 days, respectively).

As with other measurements, the rate of $bSiO_2$ export (ρ_E) was similar among most cycles. ρ_E in the shallow trap (90 or 100 m) varied from 1.24 to 2.26 mmol Si m^{-2} day^{-1} during Cycles 2−5. Very little export attenuation was observed during the transit of $bSiO_2$ to the deeper trap (150 m), as rates for these cycles at this depth ranged from 1.04 to 2.07 mmol Si m^{-2} day^{-1} (Table I). The notable exception to these results was Cycle 1, where rates in the shallow (5.90 mmol Si m^{-2} day^{-1}) and deep (6.16 mmol Si m^{-2} day^{-1}) traps were more than double those at other cycles and depths. Given $\int bSiO_2$ for the overlying waters, the turnover times of $bSiO_2$ in the upper $\sim$100 m (i.e. $\int bSiO_2/\rho_E$) are estimated by assuming insignificant $bSiO_2$ dissolution between 80 m (depth of integration) and 90−100 m (depth of shallowest traps); under a steady-state condition, turnover and net doubling times would be equal. The turnover times for Cycles 1 and 2 were $\sim$2.8 days and increased for the other cycles to 4.8−5.7 days. However, given the high variability for the doubling measurements (driven by $\int\rho_N$), the turnover times during Cycles 1−4 were statistically indistinguishable ($P > 0.3$). Only Cycle 5 turnover and doubling times were statistically different ($P = 0.02$).
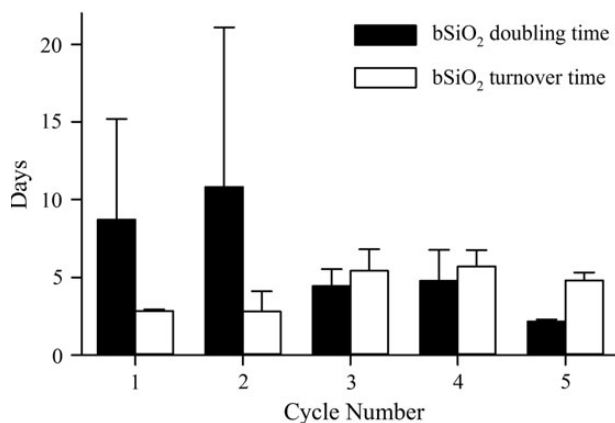
7

Fig. 4. Comparison of $bSiO_2$ accumulation (filled bars) and turnover (open bars) rates in the upper 100 m during Cycles 1–5. Calculation of rates are detailed in "Results" section. Error bars are standard deviation propagated from cycle standard deviations for $\int bSiO_2$, $\int \rho_N$ and ρ_E (see Table I).

DISCUSSION

Open-ocean comparison and the CRD silicate pump

The magnitudes of $bSiO_2$ stocks and rates ($\int bSiO_2$ stock, $\int \rho_N$ and ρ_E) are relatively high in the CRD compared with other mid- and low-latitude open-ocean systems (Table II), but are an order of magnitude lower than coastal upwelling systems or the Southern Ocean (Brzezinski et al., 2001, 2003). The range of $\int bSiO_2$ observed during our CRD cruise is similar to that measured for diatom blooms in north Atlantic mesoscale eddies (Brzezinski and Nelson, 1989; Krause et al., 2010b), oligotrophic diatom blooms near the north Pacific subtropical front (Krause et al., 2013b) and in tropical instability waves in the eastern equatorial Pacific upwelling region (Demarest et al., 2011; Krause et al., 2011). The maximum $\int \rho_N$ observed in the CRD is among the highest observed anywhere in the mid- and low-latitude open ocean, and is similar to that reported earlier (Brzezinski and Nelson, 1989) during a diatom bloom in a Gulf Stream Warm-Core ring. Similarly, the measured ρ_E in the CRD at 150 m was also among the highest reported in the low-latitude open ocean (Table II); however, there are no corresponding shallow-export data with concurrent $\int \rho_N$ measurements for the Gulf Stream Warm-Core Rings (Brzezinski and Nelson, 1989) or the eastern equatorial Pacific (Adjou et al., 2011; Demarest et al., 2011).

Despite similarities in integrated quantities to oligotrophic diatom blooms studied to date, the vertical structure of ρ_N in the CRD is unique. In many regions, vertical profiles transition from a surface water region where ρ_N is positive, to a depth or narrow zone where $\rho_N \approx 0$, followed by negative ρ_N for all deeper depths (Brzezinski and Nelson, 1989; Krause et al., 2010b, 2013b; Adjou et al., 2011; Demarest

et al., 2011). This typical vertical structure suggests that active biological accumulation occurs only in the upper euphotic zone where diatoms have ample light and typically grow fastest; therefore, the production of $bSiO_2$ exceeds its rate of dissolution. As depth increases, so does the proportion of detrital $bSiO_2$ (i.e. material transformed by passage through the food web), thus leading to an increase in the gross rate of $bSiO_2$ dissolution, with ρ_N approaching zero and then going negative. Such a two-layer character, i.e. positive ρ_N in surface and negative at depth, was not observed in the CRD. Furthermore, at depths exceeding 40 m, the rates of $bSiO_2$ production and dissolution appeared to be in balance. Because ρ_N is a net rate, it is possible (although improbable, see below) that gross $bSiO_2$ production and gross $bSiO_2$ dissolution may both be elevated to yield a near zero ρ_N at these deeper depths.

While it may be counterintuitive to have elevated production rates at depth, such a trend has been observed previously near the base of the euphotic zone or deeper (Brzezinski and Nelson, 1989). Such observations are likely due to $bSiO_2$ production being energetically inexpensive (Raven, 1983) and not directly coupled to energy derived from photosynthesis. During FLUZiE, however, the low Diatom C (Fig. 3C) and declining $bSiO_2$ standing stock at depth (Fig. 3A) argue against high diatom $bSiO_2$ production at the base of the euphotic zone. Additionally, the $bSiO_2$ material at depth did not appear to remineralize during descent between 100 and 150 m, as meaningful differences between export rates at these depths were only observed during Cycle 2 (Table I). If living diatom biomass (Fig. 3C) and [$bSiO_2$] (Fig. 3A) declined with depth, both trends suggest an increase with depth for detrital material, then why did the rate of $bSiO_2$ dissolution appear to be so low (i.e. ρ_N and ρ_E data)? We hypothesize that the unique vertical position of the CRD thermocline forms a strong silicate-pump condition.

The general "silicate-pump" model (Dugdale et al., 1995) asserts that because diatom $bSiO_2$ remineralizes less efficiently in the upper-water column than particulate organic nitrogen (PON) there is a preferential export of $bSiO_2$ out of surface waters relative to PON. For example, in a coastal system where diatoms dominate autotrophic biomass, a strong silicate-pump potentially results in silicic acid, as opposed to nitrate, being the biomass-limiting nutrient for diatoms due to low nutrient Si:N in the upwelled waters. This assumes that diatoms draw down Si and N in a ratio of 1:1 ratio (Brzezinski, 1985). In the CRD, the silicate-pump model could explain the vertical differences in the nutriclines for nitrate and silicic acid (Fig. 2D) and creates the condition where the nutrient Si:N ratio is <1 in the source-waters (>20 m). In this system, however, diatoms represent a minor fraction of the autotrophic community (Table I), and silicic acid appears unlikely to

Table II: Comparison of CRD surface silicic acid concentration (Si(OH)$_4$), integrated bSiO$_2$ standing stock ($\int$bSiO$_2$), net rates for integrated bSiO$_2$ production ($\int\rho_N$) and 150-m bSiO$_2$ export (ρ_E) to other mid- and low-latitude open ocean

System	Surface NO$_3^-$ (μM)	Surface Si(OH)$_4$ (μM)	$\int$bSiO$_2$ (mmol Si m^{-2})	$\int\rho_N$ (mmol Si m^{-2} day^{-1})	150 m ρ_E (mmol Si m^{-2} day^{-1})	References
North Atlantic Subtropical Gyre						
BATS	<0.05	0.4–1.0	1.7–3.5[a]	−1.10–0.70[a]	0.02–0.70	Krause *et al.* (Krause *et al.*, 2009b, 2010b) and Nelson and Brzezinski (Nelson and Brzezinski, 1997)
Gulf Stream Warm-Core Ring	<0.05	<0.2–2.7	5.2–47[b]	2.50–5.00[b,c]	ND	Brzezinski and Nelson (Brzezinski and Nelson, 1989) and Garside (Garside, 1985)
Mode-water eddy	<0.1	0.1–0.8	15–20[d]	0.50–0.73[d]	0.17	Buesseler *et al.* (Buesseler *et al.*, 2008) and Krause *et al.* (Krause *et al.*, 2010b)
North Pacific Subtropical Gyre						
HOT–ALOHA	<0.05	0.6–1.6	1.8–6.2[d]	0.04–0.32[c,d]	0.01–0.30	Brzezinski *et al.* (Brzezinski *et al.*, 2011)
Subtropical front summer bloom	<0.1	0.8–2.1	2.3–13[d]	−0.38–1.68[e]	0.17–0.35	Krause *et al.* (Krause *et al.*, 2013b)
Cyclone "Opal"	<0.2	<1.3	ND	ND	0.45	Benitez-Nelson *et al.* (Benitez-Nelson *et al.*, 2007)
Tropical Pacific						
Eastern equatorial upwelling	0.9–7.4	1.3–4.4	3.8–18[e]	−1.71–2.87[e]	ND	Adjou *et al.* (Adjou *et al.*, 2011), Demarest *et al.* (Demarest *et al.*, 2011) and Krause *et al.* (Krause *et al.*, 2011)
Western equatorial oligotrophic	<0.1	~1.0	2.1–3.0[a]	ND	0.04–0.12[f]	Blain *et al.* (Blain *et al.*, 1997, 1999)
Costa Rica Dome	<0.05–2.3	0.7–4.4	5.0–18	−0.73–4.19	1.04–6.16	This study

ND indicates no data.
[a]Integrated to 120 m (Blain *et al.*, 1999; Krause *et al.*, 2009b) or 140 m (other references).
[b]Integrated to 80 or 100 m (Brzezinski and Nelson, 1989).
[c]Not directly measured, also calculated as ratio of (1 − silica dissolution/silica production).
[d]Integrated to 140 m (North Atlantic) or 150 m (North Pacific).
[e]Integrated to light depth, varied 59–96 m (North Pacific) or 85–140 m (Equatorial Pacific).
[f]Export is range of values from 125 and 175 m sediment traps (Blain *et al.*, 1999).

be a biomass-limiting nutrient in the CRD mixed layer. This is supported by the nutrient Si:N in the upper 20 m of the water column being higher than in the thermocline, likely due to many organisms consuming nitrate. However, given the mixed-layer concentrations <8 μM (Fig. 2C), it is likely there was some degree of kinetic limitation for diatom Si uptake by suboptimal silicic acid (i.e. uptake at ambient silicic acid below physiological maximum, Krause *et al.*, 2012, 2015; Martin-Jezequel *et al.*, 2000). Therefore, in the CRD, where diatom biomass is considerably lower than in coastal upwelling systems, the silicate-pump condition could be maintained by altering the retention of bSiO$_2$ in the water column and increasing export efficiency.

While remineralization differences between bSiO$_2$ and PON are typical for most ocean systems (i.e. PON remineralizes faster than bSiO$_2$), we suggest that the strong and shallow thermocline of the CRD strengthens the silicate pump by slowing the physicochemical dissolution rate of bSiO$_2$. Previous studies have demonstrated that bSiO$_2$ dissolution increases between factors 2.3 and 2.6 with a 10°C temperature increase (Kamatani, 1982; Bidle *et al.*, 2002; Natori *et al.*, 2006). Given the thermocline trends during

our cruise, which are presumably representative for the CRD region during the summer season, water between 30 and 58 m was always at least 10°C cooler than surface waters (Fig. 2). Thus, at deeper depths, bSiO$_2$ dissolution would have been reduced to rates less than half those in the upper euphotic zone. Such a slowing of dissolution helps explain why 89% of our $\int\rho_N$ estimates were positive, as even lower rates of gross bSiO$_2$ production can result in net bSiO$_2$ accumulation when losses from dissolution are small. In the equatorial Pacific upwelling region, the depth at which there is a 10°C difference from the surface waters is considerably deeper, e.g. 100−200 m (Strutton *et al.*, 2011), this region has similar maximum values of $\int$bSiO$_2$ but $\int\rho_N$ are <50% those in the CRD. In the equatorial Pacific, the sinking of bSiO$_2$ particles into relatively warm subsurface waters creates a vertical zone where ρ_N is strongly negative (Adjou *et al.*, 2011; Demarest *et al.*, 2011). Consequently, ~65% of bSiO$_2$ produced in the upper euphotic zone in the equatorial Pacific is dissolved in the lower euphotic zone (Krause *et al.*, 2010a).

The broader ramification is that the CRD appears to operate as a highly efficient silicate pump, similar to a cold-water coastal upwelling system (e.g. Peru; Dugdale

et al., 1995), but with typical oligotrophic biomass. Such a situation is atypical for most open-ocean regions where diatom biomass is greatly reduced. In the North Pacific subtropical gyre, Brzezinski et al. (Brzezinski et al., 2011) observed that despite low $bSiO_2$ production relative to the North Atlantic subtropical gyre, the export was similar (Table II), suggesting this region was very efficient for exporting Si from the euphotic zone. In the CRD, $\int bSiO_2$ is 3-fold higher than and the lowest and highest rates of export are 10- to 60-fold higher than those in the North Pacific subtropical gyre (Table II). Thus, relative to low- and mid-latitude open-ocean regions, the CRD appears to be unique in its efficiency of removing Si from the euphotic zone.

Given the measured $\int \rho_N$, the high calculated $\int$Ave V_{NET} and the inferred low dissolution rates, the CRD may be a system where gross $bSiO_2$ production is fueled predominantly ($>70\%$) by newly supplied silicic acid to the euphotic zone (Brzezinski et al., 2003). This combination of factors would favor sustained, high export of $bSiO_2$ throughout the water column. This interpretation is consistent with the model results (Honjo et al., 2008) that show that $bSiO_2$ export at 2 km in the CRD is among the highest rates of any mid- or low-latitude deep-water system, comparable with rates in the cold-tongue of the eastern equatorial Pacific, offshore areas of the Peru upwelling region and the Arabian Sea. Hence, lowered $bSiO_2$ dissolution in surface waters, which appears to set up a strong silicate-pump condition, suggests a stronger efficiency of diatom $bSiO_2$ export from the euphotic zone, which could contribute to the elevated deep-water export of $bSiO_2$ in this region compared with other low-latitude systems (Honjo et al., 2008). A caveat to such an interpretation is that we cannot address the potential role of radiolarians (i.e. non-diatom siliceous plankton) to deep export. Thus, the partitioning of the relative importance of more efficient diatom $bSiO_2$ export versus increased radiolarian contribution to the deep-export rates cannot be determined with the present data and should be examined in future studies.

Food-web controls on $bSiO_2$

There were strong similarities in biological stocks and rates among the FLUZiE-cruise cycles (Table I). While diatom biomass, by C (Table I) and fucoxanthin (Selph et al., this issue) proxies, was very low, their gross growth rates were the highest among phytoplankton groups. Coupling these data with this present analysis sheds light on the transformation and fate of $bSiO_2$ during this cruise.

Food-web processes quantified during the cruise appear to have shaped the silicate-pump condition. With the exception of Cycle 5, a balanced state was observed in the upper-water column, where the net rate of accumulation for $bSiO_2$ was statistically indistinguishable (due to high variability) from its net rate of loss (Fig. 4). During Cycles 3 and 4, Diatom C was relatively high and the average $\int bSiO_2$ increased modestly above that observed during Cycle 5, the lowest cycle mean. Rates of $\int$Ave V_{NET} during Cycles 3 and 4 were also elevated (0.17 and 0.24 day^{-1}, Table I). These net rates are higher than specific rates of gross $bSiO_2$ production in open-ocean gyre systems (e.g. $0.07-0.15\ day^{-1}$, Brzezinski et al., 2011; 0.14 day^{-1}, Krause et al., 2011), indicating elevated diatom activity during these cycles, which is consistent with diatom growth rate results during this cruise (Selph et al., this issue). Diatom biomass was predominantly grazed and controlled by mesozooplankton, as 83% of diatom production in this region escapes grazing by microzooplankton (Landry et al., this issue-b; Selph et al., this issue). Additionally, Décima et al. (Décima et al., this issue) observed a tight coupling between the rate of mesozooplankton grazing and the integrated $\int \rho_N$ among the cycles.

Mesozooplankton grazing on diatoms appears to be an important ecological interaction for sustaining the active silicate pump. The tight coupling between the net rate of diatom $bSiO_2$ production and the rate of mesozooplankton grazing (Décima et al., this issue) suggests that the primary means by which diatom $bSiO_2$ is transported below the thermocline (e.g. >40 m) are within fecal pellets, as opposed to the settling of single cells. This movement of diatom $bSiO_2$ below the thermocline by transport in fecal pellets is a key ecological mechanism to moving $bSiO_2$ into the lower-temperature waters that reduce the rate of remineralization. Stukel et al. (Stukel et al., 2013a) observed that mesozooplankton fecal pellets in the CRD remineralize primarily in the euphotic zone (e.g. typically $44-52$ m). Because of the shallow thermocline (e.g. $20-40$ m), the rate of $bSiO_2$ remineralization would reduce by a factor of $2.3-2.6$ within the thermocline during descent. Hence, despite the extensive organic matter remineralization of fecal pellet material in the euphotic zone, $bSiO_2$ would still be efficiently transported to depth by this grazing mechanism. The net effect of these food-web processes and the thermocline is the enrichment of the $bSiO_2$:POC in exported particles (compare export values from Tables I and III) and a strong silicate-pump condition.

Diatom contributions to production and organic matter export

Diatom new production can be estimated using nitrate uptake and $\int \rho_N$ as follows: Diatom $\% \int \rho NO_3^- = [100 \times \int \rho_N/(Si:N \times \int \rho NO_3^-)] \times f$-ratio. This calculation will be

Table III: Estimate of percent diatom contributions to new production and POC export using surface–40 m integrated rates of net $bSiO_2$ production ($\int\rho_N$) and nitrate uptake ($\int\rho NO_3^-$, i.e. new production) and 100-m POC export (ρ_{POC})

Cycle	40-m $\int\rho_N$ (mmol Si m^{-2} day^{-1})	40-m $\int\rho NO_3^-$ (mmol NO$_3^-$ m^{-2} day^{-1})			ρ_{POC} export (mmol C m^{-2} day^{-1})	
		Total rate	Community *f*-ratio	%Diatom	Rate	%Diatom
1	2.05 ± 1.31	2.42 ± 0.32	0.53	44.9 ± 29.3%	10.0 ± 0.69	ND
2	0.63 ± 0.61	5.05 ± 1.38	0.40	5.0 ± 5.0%	5.32 ± 1.52	3.8 ± 2.2%
3	2.01 ± 0.52	2.65 ± 0.42	0.24	18.3 ± 5.5%	5.61 ± 0.43	5.0 ± 2.3%
4	1.20 ± 0.58	3.57 ± 1.05	0.32	10.8 ± 6.1%	4.19 ± 0.47	6.2 ± 1.9%
5	2.42 ± 0.14	6.11 ± 0.52	0.48	19.1 ± 2.0%	6.03 ± 0.51	7.9 ± 0.9%

The community *f*-ratio estimates the fraction of diatom N production fueled by nitrate, Cycle-average values from Stukel *et al.* (Stukel *et al., this issue*). Error terms are propagated from original measurements. ND indicates no Diatom C available for conversion of export rates.

conservative as $\int\rho_N$ will almost always be lower than gross $bSiO_2$ production—which was not measured. Integrated rates are confined to the upper 40 m, which was observed to account for 93% of the primary production rates for the full euphotic zone (Landry *et al., this issue-b*). We assume a value of Si:N ~1.0 (Brzezinski, 1985), and in the eastern equatorial Pacific this average ratio was 0.98 (directly measured) for the numerically dominant diatom groups during two different years (Krause *et al.*, 2011). The *f*-ratio, the proportion of total primary production fueled by "new" N sources (e.g. NO$_3$), was derived by converting nitrate uptake to C using C:N 6.6, and dividing by concurrently measured primary production (Table III; Stukel *et al., this issue*). The caveat is that such a value could be conservative since diatoms and other large phytoplankton in the tropical Pacific may have *f*-ratios up to 0.6 (Dugdale *et al.*, 2007).

Despite being a minor component of total autotrophic biomass, the calculated contribution of diatoms to community new production is significant (Table III). Diatoms accounted for between 5 and 45% of community new production, with a cruise mean of 19.6 ± 26.7% (SE), and the high proportional variability in Cycles 1 and 2 for $\int\rho_N$ propagates in the cruise mean. Landry *et al.* (Landry *et al., this issue-b*) estimated that the average rate of diatom primary production during this cruise was 31 ± 10 (SE) mg C m^{-2} day^{-1}, which excluded Cycle 1. By assuming a C:N of 6.6 and the mean diatom *f*-ratio of 0.36 (average for Cycles 2–5), the Landry *et al.* (Landry *et al., this issue-b*) data suggest that diatoms account for a lower fraction of new production, 3.2 ± 1.2%, than estimated here (Table III). If we, as in Landry *et al.*, also exclude Cycle 1 and use a similar strategy for conversion with the data (i.e. average of the cruise mean diatom primary production and total nitrate uptake), the cruise-averaged contribution using our $\int\rho_N$ conversion would be 13.3%—still multiple factors higher than 3.2%. Both of these calculation approaches demonstrate that the diatom contribution to new production appears to be minor in this system despite the occurrence of substantial biomass in high trophic levels (Décima *et al., this issue*), which is generally thought to be sustained by efficient trophic transfer of diatom production up the food chain. However, even the lower estimate based on the diatom carbon production data suggests that, relative to their contribution to autotrophic biomass, diatoms contribution to new production is at least multiple factors higher.

The degree of difference between rates based on converting $\int\rho_N$ and carbon-based measurements highlights a unique finding. In a previous study in the equatorial Pacific, carbon-based net diatom production conversions to Si and independent $\int\rho_N$ measurements were closely matched (Krause *et al.*, 2010a). During FLUZiE, the ratio of net carbon-based diatom production, 2.17 mmol C m^{-2} day^{-1} (Landry *et al., this issue-b*) to net $bSiO_2$ production (1.57 mmol Si m^{-2} day^{-1}, average of values in Table III) in the upper 40 m was 1.38 ± 0.54; this ratio theoretically estimates the C:Si stoichiometry of active diatoms. However, nutrient-replete diatoms have a C:Si typically ~7.7 (Brzezinski, 1985), which suggests that the C:Si in the CRD is very low. Such low ratios are symptomatic of diatom growth being severely limited by trace metals (Brzezinski *et al.*, 2015), which can result in lower diatom C (or N) quotas and higher silica per cell due to prolonging the cell-cycle phase of Si uptake. Selph *et al.* (Selph *et al., this issue*) clearly observed that diatom growth was high, nearly two doublings per day, suggesting that growth limitation was not a factor. Hence, it appears there was a surplus of $bSiO_2$ produced relative to what would be expected for replete and fast-growing diatoms.

The apparent excess net $bSiO_2$ produced may be explained if other siliceous phytoplankton were active. If so, this could also reconcile the 4-fold difference between the two estimates (3.2 versus 13.3%, see above) of diatom contributions to new production. Baines *et al.* (Baines *et al.*, 2012) demonstrated that field and laboratory cells of *Synechococcus* can accumulate Si. While Si per cell in

Synechococcus is typically in amol Si amounts, considerably lower than for diatoms ($\sim$100 s fmol to pmol), *Synechococcus* biomass was 26-fold higher than diatoms on this cruise (Landry *et al.*, this issue-b). Currently, the form of Si associated with *Synechococcus* is unknown, but if it is a particulate phase and not prone to rapid remineralization, it may represent an important term in the measured $\int \rho_N$. Another explanation is the presence of radiolarian contribution to net $bSiO_2$ production. However, their abundance, biomass and growth rates are seldom measured and are not available for this cruise. Regardless of the mechanism, we clearly observe a decoupling between the net diatom carbon produced and an apparent "overproduction" of $bSiO_2$ which does not appear to be related to growth limitation of diatoms, as has been previously observed. Such a unique result will require more focused examination in the future.

Estimating the diatom contribution to organic matter export involves a similar approach as above: Diatom %POC export $= 100 \times \rho_E / [\text{Si:C} \times \rho_{POC}]$. Such calculations are influenced heavily by the Si:C ratio used for diatom-associated organic matter. As with the new production estimation, a nutrient-replete diatom Si:C ratio can be used (Nelson and Brzezinski, 1997), but this results in calculated diatom export being 150–450% of measured POC export (data not shown). This significant overestimate presents a strong argument that the $bSiO_2$ captured in sediment traps is not in the form of intact diatoms. Assuming that this material is well mixed in the water column and that empty frustules and living diatoms are equally likely to be grazed or incorporated into aggregates (i.e. detritus), we can calculate Si:C using the ratio of $[bSiO_2]$:[Diatom C] measured during the cycles (Table I; Krause *et al.*, 2015).

Based on data from Cycles 2–5, where [Diatom C] data are available, we estimate that diatoms contributed between 3.8 and 7.9% of total organic matter export, both suggest a disproportionately high contribution relative to their low proportion of autotrophic biomass (Table III). In Cycles 2 and 4, the calculated contributions of diatoms to new production and organic matter export are similar or within error estimates. However, in Cycles 3 and 5, the contributions to new production were clearly higher than to organic matter export. Stukel *et al.* (Stukel *et al.*, 2013a) examined diatoms in the same sediment traps and observed diatom organic C to be even lower (< 0.6% for all cycles), suggesting the direct sinking of diatoms was minor. With the caveat that production and export can be temporally separated, the difference between relatively high contributions to water-column new production for diatoms and a lower observed contributions to export is consistent with strong food-web transformation of diatom organic matter in the water column prior to export. This was clearly observed in half the cycles whereas low rates and/or high proportional variability (e.g. Cycles 2 and 4) demonstrates that this condition is variable and the contributions of diatoms to both processes are similar (Table III). Conclusions from recent studies in Southern California (Krause *et al.*, 2015) and the North Atlantic (Amacher *et al.*, 2013) also demonstrate that diatom contribution to organic matter export was low while the Southern California study observed the same trend of higher diatom contribution to new production. Thus, the indication that diatoms have a disproportionately high contribution to new production and organic matter export (e.g. Nelson and Brzezinski, 1997; Krause *et al.*, 2009b; Brzezinski *et al.*, 2011) may require revision. Whether the results presented here are broadly reflective of oligotrophic and/or low-latitude open-ocean regions will require future studies that couple both biogeochemical and ecological methods when assessing diatom contributions to these processes.

DATA ARCHIVING

This data and the general project datasets are available through the Biological and Chemical Oceanography Data Management Office under the project title "Costa Rica Dome FLUx and Zinc Experiments" (http://www.bco-dmo.org/project/515387).

ACKNOWLEDGEMENTS

FUNDING

REFERENCES

Adjou, M., Tréguer, P., Dumousseaud, C., Corvaisier, R., Brzezinski, M. A. and Nelson, D. M. (2011) Particulate silica and Si recycling in the surface waters of the Eastern Equatorial Pacific. *Deep-Sea Res. II*, **58**, 449–461.

Amacher, J., Neuer, S. and Lomas, M. (2013) DNA-based molecular fingerprinting of eukaryotic protists and cyanobacteria contributing to

sinking particle flux at the Bermuda Atlantic time-series study. *Deep-Sea Res. II*, **93**, 71–83.

Baines, S. B., Twining, B. S., Brzezinski, M. A., Krause, J. W., Vogt, S., Assael, D. and McDaniel, H. (2012) Significant silicon accumulation by marine picocyanobacteria. *Nat. Geosci.*, **5**, 886–891.

Benitez-Nelson, C. R., Bidigare, R. R., Dickey, T. D., Landry, M. R., Leonard, C. L., Brown, S. L., Nencioli, F., Rii, Y. M. *et al.* (2007) Mesoscale eddies drive increased silica export in the subtropical Pacific Ocean. *Science*, **316**, 1017–1021.

Bidle, K. D., Manganelli, M. and Azam, F. (2002) Regulation of oceanic silicon and carbon preservation by temperature control on bacteria. *Science*, **298**, 1980–1984.

Blain, S., Leynaert, A., Tréguer, P., Chretiennotdinet, M. J. and Rodier, M. (1997) Biomass, growth rates and limitation of Equatorial Pacific diatoms. *Deep-Sea Res. I*, **44**, 1255–1275.

Blain, S., Tréguer, P. and Rodier, M. (1999) Stocks and fluxes of biogenic silica in the western oligotrophic equatorial Pacific. *J. Geophys. Res. Oceans*, **104**, 3357–3367.

Brzezinski, M. A. (1985) The Si:C:N ratio of marine diatoms: Interspecific variability and the effect of some environmental variables. *J. Phycol.*, **21**, 347–357.

Brzezinski, M. A., Jones, J. L., Bidle, K. D. and Azam, F. (2003) The balance between silica production and silica dissolution in the sea: Insights from Monterey Bay, California, applied to the global data set. *Limnol. Oceanogr.*, **48**, 1846–1854.

Brzezinski, M. A., Krause, J. W., Bundy, R. M., Barbeau, K. A., Franks, P. J. S., Goericke, R., Landry, M. R. and Stukel, M. R. (2015) Variable influence of iron stress on siliceous biomass and silica production and silicon and carbon export in a frontal zone within the California Current. *J. Geophys. Res. Oceans*. doi:10.1002/2015JC010829.

Brzezinski, M. A., Krause, J. W., Church, M. J., Karl, D. M., Li, B., Jones, J. L. and Updyke, B. (2011) The annual silica cycle of the North Pacific subtropical gyre. *Deep-Sea Res. I*, **58**, 988–1001.

Brzezinski, M. A. and Nelson, D. M. (1989) Seasonal changes in the silicon cycle within a Gulf Stream warm-core ring. *Deep-Sea Res.*, **36**, 1009–1030.

Brzezinski, M. A. and Nelson, D. M. (1995) The annual silica cycle in the Sargasso Sea near Bermuda. *Deep-Sea Res. I*, **42**, 1215–1237.

Brzezinski, M. A., Nelson, D. M., Franck, V. M. and Sigmon, D. E. (2001) Silicon dynamics within an intense open-ocean diatom bloom in the Pacific sector of the Southern Ocean. *Deep-Sea Res. II*, **48**, 3997–4018.

Buesseler, K. O., Lamborg, C., Cai, P., Escoube, R., Johnson, R., Pike, S., Masque, P., Mcgillicuddy, D. *et al.* (2008) Particle fluxes associated with mesoscale eddies in the Sargasso Sea. *Deep-Sea Res. II*, **55**, 1426–1444.

Campbell, L. and Vaulot, D. (1993) Photosynthetic picoplankton community structure in the subtropical North Pacific Ocean near Hawaii (station ALOHA). *Deep-Sea Res. I*, **40**, 2043–2060.

Décima, M., Landry, M. R., Stukel, M. R., Lopez-Lopez, L. and Krause, J. W. (this issue) Mesozooplankton biomass and grazing in the Costa Rica Dome: amplifying variability through the plankton food web. *J. Plankton Res.* (in review).

Demarest, M. S., Brzezinski, M. A., Nelson, D. M., Krause, J. W., Jones, J. L. and Beucher, C. P. (2011) Net biogenic silica production and nitrate regeneration determine the strength of the silica pump in the Eastern Equatorial Pacific. *Deep-Sea Res. II*, **58**, 462–476.

Devol, A. H. (2008) Denitrification including Anammox. In Capone, D. G., Bronk, D. A., Mulholland, M. R. and Carpenter, E. J. (eds), *Nitrogen in the Marine Environment*. 2nd edn. Academic Press, pp. 263–301.

Dugdale, R. C. and Goering, J. J. (1967) Uptake of new and regenerated forms of nitrogen in primary productivity. *Limnol. Oceanogr.*, **12**, 196–206.

Dugdale, R. C., Wilkerson, F. P., Chai, F. and Feely, R. (2007) Size-fractionated nitrogen uptake measurements in the equatorial Pacific and confirmation of the low Si-high-nitrate low-chlorophyll condition. *Global Biogeochem. Cycles*, **21**, 10.

Dugdale, R. C., Wilkerson, F. P. and Minas, H. J. (1995) The role of a silicate pump in driving new production. *Deep-Sea Res. II*, **42**, 697–719.

Durand, M. D., Olson, R. J. and Chisholm, S. W. (2001) Phytoplankton population dynamics at the Bermuda Atlantic Time-series station in the Sargasso Sea. *Deep-Sea Res. II*, **48**, 1983–2003.

Franck, V. M., Bruland, K. W., Hutchins, D. A. and Brzezinski, M. A. (2003) Iron and zinc effects on silicic acid and nitrate uptake kinetics in three high-nutrient, low-chlorophyll (HNLC) regions. *Mar. Ecol. Prog. Ser.*, **252**, 15–33.

Garside, C. (1985) The vertical distribution of nitrate in open ocean surface water. *Deep-Sea Res.*, **32**, 723–732.

Goldthwait, S. A. and Steinberg, D. K. (2008) Elevated biomass of mesozooplankton and enhanced fecal pellet flux in cyclonic and mode-water eddies in the Sargasso Sea. *Deep-Sea Res. II*, **55**, 1360–1377.

Honjo, S., Manganini, S. J., Krishfield, R. A. and Francois, R. (2008) Particulate organic carbon fluxes to the ocean interior and factors controlling the biological pump: a synthesis of global sediment trap programs since 1983. *Prog. Oceanogr.*, **76**, 217–285.

Kamatani, A. (1982) Dissolution rates of silica from diatoms decomposing at various temperatures. *Mar. Biol.*, **68**, 91–96.

Krause, J. W., Brzezinski, M. A., Goericke, R., Landry, M. R., Ohman, M. D., Stukel, M. R. and Taylor, A. G. (2015) Variability in diatom contributions to biomass, organic matter production, and export across a frontal gradient in the California Current Ecosystem. *J. Geophys. Res. Oceans*, **120**, 1032–1047.

Krause, J. W., Brzezinski, M. A., Landry, M. R., Baines, S. B., Nelson, D. M., Selph, K. E., Taylor, A. G. and Twining, B. S. (2010a) The effects of biogenic silica detritus, zooplankton grazing, and diatom size structure on silicon cycling in the euphotic zone of the eastern equatorial Pacific. *Limnol. Oceanogr.*, **55**, 2608–2622.

Krause, J. W., Brzezinski, M. A., Siegel, D. A. and Thunell, R. C. (2013a) Biogenic silica standing stock and export in the Santa Barbara Channel ecosystem. *J. Geophys. Res. Oceans*, **118**, 736–749.

Krause, J. W., Brzezinski, M. A., Villareal, T. A. and Wilson, C. (2012) Increased kinetic efficiency for silicic acid uptake as a driver of summer diatom blooms in the North Pacific Subtropical Gyre. *Limnol. Oceanogr.*, **57**, 1084–1098.

Krause, J. W., Brzezinski, M. A., Villareal, T. A. and Wilson, C. (2013b) Biogenic silica cycling during summer phytoplankton blooms in the North Pacific subtropical gyre. *Deep-Sea Res. I*, **71**, 49–60.

Krause, J. W., Lomas, M. W. and Nelson, D. M. (2009a) Biogenic silica at the Bermuda Atlantic Time-series Study site in the Sargasso Sea: temporal changes and their inferred controls based on a 15-year record. *Global Biogeochem. Cycles*, **23**, GB3004.

Krause, J. W., Nelson, D. M. and Brzezinski, M. A. (2011) Biogenic silica production and the diatom contribution to primary production

and nitrate uptake in the eastern equatorial Pacific Ocean. *Deep-Sea Res. II*, **58**, 434–448.

Krause, J. W., Nelson, D. M. and Lomas, M. W. (2009b) Biogeochemical responses to late-winter storms in the Sargasso Sea, II: increased rates of biogenic silica production and export. *Deep-Sea Res. I*, **56**, 861–874.

Krause, J. W., Nelson, D. M. and Lomas, M. W. (2010b) Production, dissolution, accumulation and potential export of biogenic silica in a Sargasso Sea mode-water eddy. *Limnol. Oceanogr.*, **55**, 569–579.

Landry, M. R., Décima, M., Simmons, M. P., Hannides, C. C. S. and Daniels, E. (2008) Mesozooplankton biomass and grazing responses to Cyclone Opal, a subtropical mesoscale eddy. *Deep-Sea Res. II*, **55**, 1378–1388.

Landry, M. R., de Verneil, A., Goes, J. I. and Moffett, J. W. (this issue-a) Plankton dynamics and biogeochemical fluxes in the Costa Rica Dome: introduction to the CRD Flux and Zinc experiments. *J. Plankton Res.* (in review).

Landry, M. R., Ohman, M. D., Goericke, R., Stukel, M. R., Barbeau, K. A., Bundy, R. and Kahru, M. (2012) Pelagic community responses to a deep-water front in the California Current Ecosystem: overview of the A-Front Study. *J. Plankton Res.*, **34**, 739–748.

Landry, M. R., Ohman, M. D., Goericke, R., Stukel, M. R. and Tsyrklevich, K. (2009) Lagrangian studies of phytoplankton growth and grazing relationships in a coastal upwelling ecosystem off Southern California. *Prog. Oceanogr.*, **83**, 208–216.

Landry, M. R., Selph, K. E., Décima, M., Gutiérrez-Rodríguez, A., Stukel, M. R., Taylor, A. G. and Pasulka, A. L. (this issue-b) Phytoplankton production and grazing balances in the Costa Rica Dome. *J. Plankton Res*. (in review).

Leynaert, A., Treguer, P., Lancelot, C. and Rodier, M. (2001) Silicon limitation of biogenic silica production in the Equatorial Pacific. *Deep-Sea Res. I*, **48**, 639–660.

Li, W., Rao, S., Harrison, W., Smith, J., Cullen, J., Irwin, B. and Platt, T. (1983) Autotrophic picoplankton in the tropical ocean. *Science*, **219**, 292–295.

Martin-Jezequel, V., Hildebrand, M. and Brzezinski, M. A. (2000) Silicon metabolism in diatoms: Implications for growth. *J. Phycol.*, **36**, 821–840.

Natori, Y., Haneda, A. and Suzuki, Y. (2006) Vertical and seasonal differences in biogenic silica dissolution in natural seawater in Suruga Bay, Japan: Effects of temperature and organic matter. *Mar. Chem.*, **102**, 230–241.

Nelson, D. M. and Brzezinski, M. A. (1997) Diatom growth and productivity in an oligotrophic midocean gyre: a 3-yr record from the Sargasso Sea near Bermuda. *Limnol. Oceanogr.*, **42**, 473–486.

Pennington, J. T., Mahoney, K. L., Kuwahara, V. S., Kolber, D. D., Calienes, R. and Chavez, F. P. (2006) Primary production in the eastern tropical Pacific: a review. *Prog. Oceanogr.*, **69**, 285–317.

Raven, J. A. (1983) The transport and function of silicon in plants. *Biol. Rev.*, **58**, 179–207.

Selph, K. E., Landry, M. R., Taylor, A. G., Gutiérrez-Rodríguez, A., Stukel, M. R., Wokuluk, J. and Pasulka, A. (this issue) Phytoplankton production and taxon-specfici growth rates in the Costa Rica Dome. *J. Plankton Res*. (in review).

Strickland, J. D. H. and Parsons, T. R. (1972) *A Practical Handbook of Seawater Analysis*. Bulletin of the Fisheries Research Board of Canada, Ottawa.

Strutton, P. G., Palacz, A. P., Dugdale, R. C., Chai, F., Marchi, A., Parker, A. E., Hogue, V. and Wilkerson, F. P. (2011) The impact of equatorial Pacific tropical instability waves on hydrography and nutrients: 2004–2005. *Deep-Sea Res. II*, **58**, 284–295.

Stukel, M. R., Benitez-Nelson, C. R., Décima, M., Taylor, A. G., Buchwald, C. and Landry, M. R. (this issue) The biological pump in the Costa Rica Dome: an open ocean upwelling system with high new production and low export. *J. Plankton Res*. (in review).

Stukel, M. R., Décima, M., Selph, K. E., Taniguchi, D. A. and Landry, M. R. (2013a) The role of *Synechococcus* in vertical flux in the Costa Rica upwelling dome. *Prog. Oceanogr.*, **112**, 49–59.

Stukel, M. R., Ohman, M. D., Benitez-Nelson, C. R. and Landry, M. R. (2013b) Contributions of mesozooplankton to vertical carbon export in a coastal upwelling system. *Mar. Ecol. Prog. Ser.*, **491**, 47–65.

Taylor, A. G., Landry, M. R., Freibiott, A., Selph, K. E. and Gutiérrez-Rodríguez, A. (this issue) Phytoplankton community biomass, composition and HPLC diagnostic pigments in the Costa Rica upwelling dome. *J. Plankton Res*. (in review).